EUMETSAT Satellite Application Facility on Climate Monitoring

The EUMETSAT
Network of
Satellite
Application
Facilities

CM SAF
Climate Monitoring

Product User Manual

SEVIRI cloud products

CLAAS Edition 2

Fractional Cloud Cover	**CM-21011**
Joint Cloud property Histogram	**CM-21021**
Cloud Top level	**CM-21031**
Cloud Phase	**CM-21041**
Liquid Water Path	**CM-21051**
Ice Water Path	**CM-21061**

Reference Number:	SAF/CM/KNMI/PUM/SEV/CLD
Issue/Revision Index:	2.2
Date:	12.04.2018

Document Signature Table

	Name	**Function**	**Signature**	**Date**
Author	Stephan Finkensieper	CM SAF scientist (DWD)		20/04/2016
	Timo Hanschmann	CM SAF scientist (DWD)		10/06/2016
	Martin Stengel	CM SAF scientist (DWD)		
	Nikos Benas	CM SAF scientist (KNMI)		
	Gerd-Jan van Zadelhoff	CM SAF scientist (KNMI)		
	Jan Fokke Meirink	CM SAF scientist (KNMI)		
Editor	Jan Fokke Meirink	CM SAF scientist (KNMI)		20/06/2016
Approval	Rainer Hollmann	Science Coordinator		12/04/2018
Release	Martin Werscheck	Project Manager		

Distribution List

Internal Distribution	
Name	**No. Copies**
DWD Archive	1
CM SAF Team	1

External Distribution		
Company	**Name**	**No. Copies**
PUBLIC		1

Document Change Record   3

Issue/ Revision	Date	DCN No.	Changed Pages/Paragraphs
1.0	20/04/2016	SAF/CM/KNMI/PUM/SEV/CLD/2/1.0	First official version submitted for DRR 2.4
2.1	10/06/2016	SAF/CM/KNMI/PUM/SEV/CLD/2.1	Modified version addressing DRR 2.4 RIDs. In addition, a number of corrections to Section 8 where made.
2.2	12/04/2018	SAF/CM/KNMI/PUM/SEV/CLD/2.2	Editorial update page 28

Table of Contents

List of Figures

List of Tables

Applicable documents

Reference	Title	Code
AD 1	EUMETSAT CM SAF CDOP 2 Product Requirements Document (PRD)	SAF/CM/DWD/PRD/2.7

Reference documents

Reference	Title	Code
RD 1	Validation Report SEVIRI Cloud Products Edition 2 (CLAAS-2)	SAF/CM/KNMI/VAL/SEV/CLD/2.1
RD 2	Algorithm Theoretical Basis Document SEVIRI cloud products processing chain	SAF/CM/DWD/ATBD/SEV/CLD/2.3
RD 3	Algorithm Theoretical Basis Document SEVIRI cloud physical products	SAF/CM/KNMI/ATBD/SEV/CPP/2.2
RD 4	Algorithm Theoretical Basis Document SAFNWC/MSG "Cloud mask, Cloud Type, Cloud Top Temperature, Pressure, Height"	SAF/NWC/CDOP/MFL/SCI/ATBD/01, v3.2
RD 5	Algorithm Theoretical Basis Document Joint Cloud property Histograms AVHRR/SEVIRI	SAF/CM/SMHI/ATBD/JCH/2.0

1   The EUMETSAT SAF on Climate Monitoring (CM SAF)

The importance of climate monitoring with satellites was recognized in 2000 by EUMETSAT Member States when they amended the EUMETSAT Convention to affirm that the EUMETSAT mandate is also to "contribute to the operational monitoring of the climate and the detection of global climatic changes". Following this, EUMETSAT established within its Satellite Application Facility (SAF) network a dedicated centre, the SAF on Climate Monitoring (CM SAF, http://www.cmsaf.eu).

The consortium of CM SAF currently comprises the Deutscher Wetterdienst (DWD) as host institute, and the partners from the Royal Meteorological Institute of Belgium (RMIB), the Finnish Meteorological Institute (FMI), the Royal Meteorological Institute of the Netherlands (KNMI), the Swedish Meteorological and Hydrological Institute (SMHI), the Meteorological Service of Switzerland (MeteoSwiss), and the Meteorological Service of the United Kingdom (UK MetOffice). Since the beginning in 1999, the EUMETSAT Satellite Application Facility on Climate Monitoring (CM SAF) has developed and will continue to develop capabilities for a sustained generation and provision of Climate Data Records (CDR's) derived from operational meteorological satellites.

In particular, the generation of long-term data records is pursued. The ultimate aim is to make the resulting data records suitable for the analysis of climate variability and potentially the detection of climate trends. CM SAF works in close collaboration with the EUMETSAT Central Facility and liaises with other satellite operators to advance the availability, quality and usability of Fundamental Climate Data Records (FCDRs) as defined by the Global Climate Observing System (GCOS). As a major task the CM SAF utilizes FCDRs to produce records of Essential Climate Variables (ECVs) as defined by GCOS. Thematically, the focus of CM SAF is on ECVs associated with the global energy and water cycle.

Another essential task of CM SAF is to produce data records that can serve applications related to the Global Framework of Climate Services initiated by the WMO World Climate Conference-3 in 2009. CM SAF is supporting climate services at national meteorological and hydrological services (NMHSs) with long-term data records but also with data records produced close to real time that can be used to prepare monthly/annual updates of the state of the climate. Both types of products together allow for a consistent description of mean values, anomalies, variability and potential trends for the chosen ECVs. CM SAF ECV data records also serve the improvement of climate models both at global and regional scale.

As an essential partner in the related international frameworks, in particular WMO SCOPE-CM (Sustained COordinated Processing of Environmental satellite data for Climate Monitoring), the CM SAF - together with the EUMETSAT Central Facility, assumes the role as main implementer of EUMETSAT's commitments in support to global climate monitoring. This is achieved through:

- Application of highest standards and guidelines as lined out by GCOS for the satellite data processing,

- Processing of satellite data within a true international collaboration benefiting from developments at international level and pollinating the partnership with own ideas and standards,

- Intensive validation and improvement of the CM SAF climate data records,

- Taking a major role in data record assessments performed by research organisations such as WCRP (World Climate Research Program). This role provides the CM SAF with deep contacts to research organizations that form a substantial user group for the CM SAF CDRs,

- Maintaining and providing an operational and sustained infrastructure that can serve the community within the transition of mature CDR products from the research community into operational environments.

A catalogue of all available CM SAF products is accessible via the CM SAF webpage, http:/www.cmsaf.eu/. Here, detailed information about product ordering, add-on tools, sample programs and documentation is provided.

2 Executive summary

This CM SAF Product User Manual provides information on the CLAAS-2 data record (CLAAS-2: CLoud property dAtAset using SEVIRI, edition 2) derived from Spinning Enhanced Visible and InfraRed Imager (SEVIRI) observations onboard the EUMETSAT METEOSAT Second Generation (MSG) satellites. CLAAS-2 is the next edition of CLAAS (Stengel et al. 2014). The covered time period of CLAAS-2 ranges from beginning of 2004 to December of 2015, thus includes MSG-1, MSG-2 and MSG-3 for which the transitions took place in April 2007 and January 2013.

The CLAAS-2 data record contains multiple cloud parameters derived from SEVIRI. The CM SAF release of CLAAS-2 contains the following cloud variables:

> Fractional Cloud Cover [CM-21011, CFC]
> Joint Cloud property histogram [CM-21021, JCH]
> Cloud Top level [CM-21031, CTO]
> Cloud Phase [CM-21041, CPH]
> Liquid Water Path [CM-21051, LWP]
> Ice Water Path [CM-21061, IWP]

Some attractive features of the CLAAS-2 data record are:
- All atmospheric quantities describing a cloudy atmosphere are highly variable on both, spatial as well as temporal scales. The temporal and spatial resolution of SEVIRI allows a sufficient sampling of every pixel of the SEVIRI disc and can therefore provide accurate estimates of daily and monthly averages of the highly fluctuating quantities. Also, the diurnal cycle of the observed quantities can be described properly which provides further insight into the processes of cloud formation and atmospheric motion. It can also be seen as complementary information to the long-term global cloud property datarecords, e.g. CLARA, PATMOS-X, MODIS, ISCCP, with its capability of resolving diurnal cycles, thus providing corresponding uncertainty estimates or even correction in this respect for data records being exclusively based on polar orbiters.
- The SEVIRI field of view covers a fairly large domain of the globe. For the regions covered (e.g. Europe, Africa, Atlantic Ocean) this allows monitoring climate variability of the considered cloud properties, which becomes more and more mature with SEVIRI's growing measurement record (12 years in this data record).
- The data record is characterized by a very fine spatial resolution of approximately 3 (near the sub-satellite point) to 5 km (e.g. over Europe). This fine resolution is kept in the Level 2 products (on original SEVIRI projection and resolution), but also in the Level 3 products (mapped onto a latitude-longitude grid with 0.05° spatial resolution). With this, also small scale weather and climate features can be resolved and investigated.

CLAAS-2 features many improvements and advantages compared to its first edition, some of the most important ones being:
- The length of the record is 12 years instead of 8 years. Given the good stability of the SEVIRI instrument and the CLAAS-2 record, this is approaching a typical length required for trend analyses.

- The temporal resolution of the level-2 data is 15 minutes rather than 1 hour. This gives both a better description of diurnal cycles and better sampling rates for aggregated products.
- CLAAS-2 features various algorithm improvements for all cloud parameters. Particularly, the CPH algorithm has dramatically improved.
- More cloud parameters are provided as additional layers, which were not provided for CLAAS-1. An example is cloud particle effective radius.

This manual briefly describes the historical development of CM SAF, the CLAAS-2 data record and the versioning for CLAAS-2 products. A technical description of the data records including information on the file format as well as on the data access is provided. Furthermore, details on the implementation of the retrieval processing chain, and individual algorithm descriptions are available in the algorithm theoretical basis documents [RD 2] - [RD 5]. Basic accuracy requirements are defined in the product requirements document [AD 1]. A detailed validation of the SEVIRI based parameters is available in the validation report [RD 1].

3 Compilation of the CLAAS-2 cloud data record

The CLAAS-2 data record is based on 12 years of SEVIRI measurements. SEVIRI is a passive visible and infrared imager mounted on the Meteosat Second Generation (MSG) satellites 1 to 4. These are geostationary satellites which, by their rotation, support a SEVIRI imaging repeat cycle of 15 minutes. SEVIRI itself is an optical imaging radiometer with 12 spectral channels ranging from the visible (approx. 0.6 µm) to the infrared of about 13.4 µm. The respective MSGs in operational mode are centred near 0°/0° latitude/longitude, where a full earth disk image includes Europe, Africa, the Middle East and the Atlantic Ocean. The horizontal resolution of a SEVIRI image is 3 x 3 km² at nadir. CLAAS-2 covers the time-span 2004-2015, and is based on measurements of MSG-1, MSG-2 and MSG-3 (see Figure 3-1). Gaps of more than 24 hours in the prime satellite were filled by a back-up satellite. For the derivation of our cloud products we used the Level 1.5 SEVIRI data provided by EUMETSAT. The Level 1.5 data record comprises images that have already undergone certain modifications by EUMETSAT: they have been corrected for all unwanted radiometric and geometric effects, geolocated using a standardised projection, and calibrated and radiance-linearised. Because of the introduction of a new radiance definition by EUMETSAT on 5 May 2008, we use reprocessed Level 1.5 data prior this date with the base algorithm version 0201 and the near real time version 0100 afterwards to ensure homogeneity of the time series.
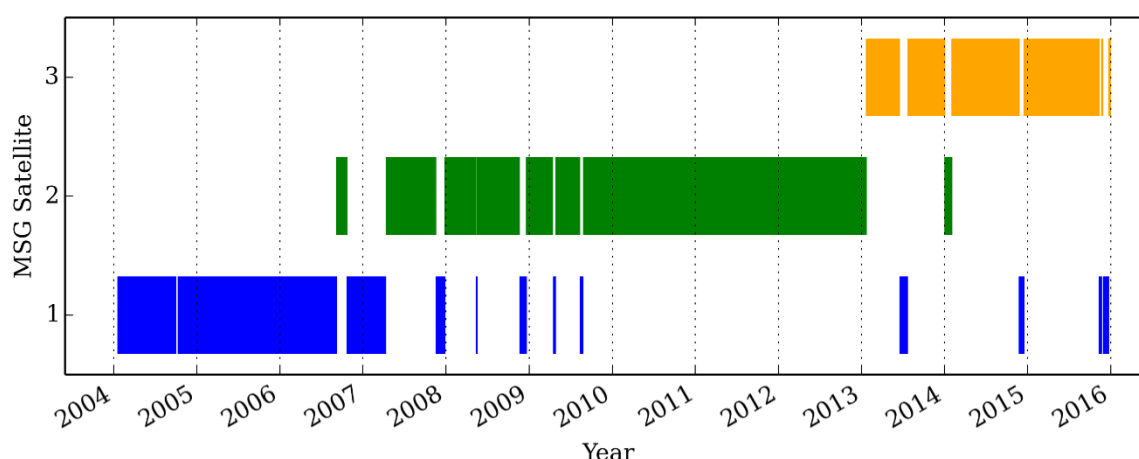
Figure 3-1: Overview of SEVIRI measurements record at CM SAF used as basis for cloud products. Short-term data gaps are shown enlarged for better visibility.

The Level 1.5 radiance data record was processed with two software packages: the MSG v2012 software package by the NWCSAF (SAF to support to Nowcasting and Very Short Range Forecasting) used to derive cloud fraction and cloud top properties (Derrien and Le Gléau, 2005; [RD 3]), and the CPP (Cloud Physical Properties) algorithm (Roebeling et al. 2006; [RD 4]), which retrieves cloud thermodynamic phase, cloud optical thickness, cloud particle effective radius, and liquid/ice water path. For processing the SEVIRI data we adopted the following strategy: processing started for each day of a specific month at midnight, all days of up to three months were processed in parallel. The first setting was necessary not only to speed up processing, but also to make temporal dependency for the cloud mask calculation possible (Derrien and LeGleau, 2010).

The time series of SEVIRI reflectances was carefully calibrated against the Moderate Resolution Imaging Spectroradiometer (MODIS), which improved especially the retrieval of

microphysical parameters. The calibration method is outlined in Meirink et al. (2013). With the calibration also homogenisation was performed because the same MODIS instrument was used for all MSG satellites. The IR radiances of SEVIRI were used as provided by EUMETSAT, relying on the on-board black-body calibration.

As shown in Figure 3-1, the prime satellite is occasionally inactive and measurements are then provided by the back-up satellite. Data from these periods (see [RD 2] for exact times) should be considered with some caution because the back-up satellite has a different position and consequently a different viewing geometry, and its shortwave calibration coefficients, being based on an extrapolation of the calibration during its functioning as prime satellite, have a larger uncertainty. A second warning must be made regarding periods with missing time slots, which will also be characterized by larger uncertainties. Information on missing data can be retrieved from the 'nobs' attributes in the product files, indicating the number of pixels and number of days used for aggregation to produce the daily and monthly mean files, respectively. Overall the number of missing time slots is low.

For a more detailed instrument specification and description of the calibration the reader is referred to the SEVIRI Algorithm Theoretical Baseline Document [RD 2].

4   Product definitions

The CLAAS-2 cloud data record from SEVIRI provides seven cloud parameters. All cloud products are introduced in Table 4-1 with associated acronyms and units.

All parameters can be accessed on Level 2 basis, which means in original SEVIRI pixel size (3 x 3 km² at sub-satellite point) and at 15-minute resolution. The products CFC, CPH, CTO, LWP, IWP are also available as daily and monthly composites on a regular latitude/longitude grid with a spatial resolution of 0.05° × 0.05° degrees. Additionally, monthly mean diurnal cycles are provided with a temporal resolution of one hour. Please note that the Joint Cloud property Histogram and the monthly mean diurnal cycle fields are only available on a 0.25° x 0.25° grid. Also, JCH is available on monthly basis only. All product features are listed in Table 4-2.

Table **4-1**: CLAAS-2 product suite.

Product identifier	Acronym	Product title	Unit (*Level 2* / Level 3)
CM-21011	CFC	Cloud Fractional Cover (or Cloud Amount)	*dimensionless* / %
CM-21031	CTO	Cloud Top information, expressed either as Cloud Top Pressure, Cloud Top Height or Cloud Top Temperature	*hPa, m or K* / hPa, m or K
CM-21041	CPH	Cloud thermodynamic Phase	*dimensionless* / %
CM-21051	LWP	Liquid Water Path	*kg/m²* / kg/m²
	COT	Liquid Cloud Optical Thickness	*dim.less* / dim.less
	REFF	Liquid Cloud particle effective radius	*μm* / μm
CM-21061	IWP	Ice Water Path	*kg/m²* / kg/m²
	COT	Ice Cloud Optical Thickness	*dim.less* / dim.less
	REFF	Ice Cloud particle effective radius	*μm* / μm
CM-21021	JCH	Joint Cloud property Histogram, based on CPH, CTP, and COT	dimensionless

Table 4-2: Level-3 product features incl. day and night separation, liquid water and ice as well as histogram representation. Please note that the LWP and IWP histograms are combined in one product (CWPmh), see sections 5.4 and 5.5.

	Daily mean	**Monthly mean**	**Monthly mean diurnal cycle**	**Monthly histograms**
CFC	✔ day/night high/mid/low	✔ day/night high/mid/low	✔	
CTO	✔	✔	✔	✔
CPH	✔ day/night liquid/ice	✔ day/night liquid/ice	✔	
LWP (+ τ, r$_e$)	✔	✔	✔	✔
IWP (+ τ, r$_e$)	✔	✔	✔	✔
JCH				✔ liquid/ice

Acknowledging the different observation capabilities during night and during day and also taking into account existing diurnal variations in cloudiness, a further separation of results into daytime and night-time portions was done for CFC. Here, all observations made under twilight conditions (solar zenith angles between 75-95 degrees) have been excluded in order to avoid being affected by specific cloud detection problems occurring in the twilight zone.

The temporal coverage of the data records ranges from mid-January 2004 to December 2015.

For each cloud parameter, also various metadata and information about selected statistical parameter distributions in each grid point is available in addition to the main product content described above. Details on how to access this information is given in Section 6.

A complete description of the retrieval methods for each individual product is given in the Algorithm Theoretical Basis Documents [RD 3, RD 4, RD 5]. The general methods for SEVIRI calibration and calculation of Level 3 products are described in [RD 2].

5   Product description

In this section, each cloud product is shortly described regarding retrieval methods, information content and limitations. Validation results are also described shortly for each cloud product. A summary of all validation results can also be found in Section 6. More details on achieved validation results are given in [RD 1]. At the end of each product description a short statement on recommended applications areas is given.

5.1   Fractional cloud cover – CFC
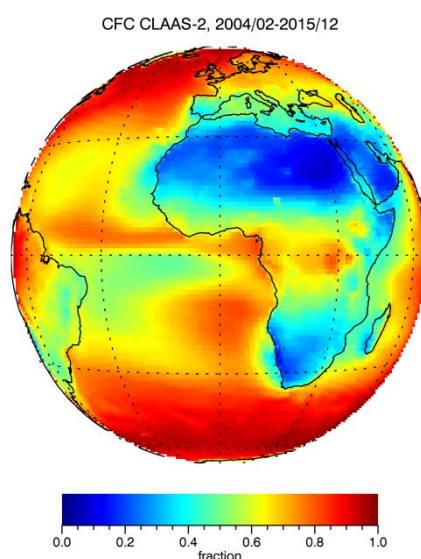
Figure 5-1: CLAAS-2 fractional cloud cover averaged from 02/2004 to 12/2015 monthly means.

The level-2 (instantaneous pixel) cloud mask comprises 6 categories: cloud free, cloud contaminated, cloud filled, undefined, snow/ice at the surface (under cloud-free conditions), and non-processed. The cloud fractional cover level-3 product (monthly and daily mean, as well as monthly mean diurnal cycle) is defined as the fraction of cloudy pixels per grid box compared to the total number of analysed pixels in the grid box. Pixels are counted as cloudy if they belong to the classes cloud filled or cloud contaminated. Fractional cloud cover is expressed in percent. As an example, the averaged fractional cloud cover from the entire CLAAS-2 period (02/2004-12/2015) is shown in in Figure 5-1. Cloud fraction is further separated into low (CTP > 680 hPa) , middle (440 hPa < CTP < 680 hPa) and high (CTP < 440 hPa) cloud cover using the CTP product from Section 5.2, as well as daytime (solar zenith angle below 75°) and nighttime (solar zenith angle above 95°) cloud cover.

Short Algorithm description

The cloud screening and cloud masking is performed using the NWC SAF MSG v2012 algorithm, which is described in more detail in [RD 3]. See http://NWC SAF.org for details on the NWC-SAF project. The algorithm is based on a multi-spectral thresholding technique applied to every pixel of the satellite scene (Derrien and Le Gléau, 2005 and 2010). Several threshold tests may be applied and must be passed before a pixel is assigned to be cloudy or cloud-free.

Thresholds are determined from present viewing and illumination conditions and from the current atmospheric state (prescribed by data assimilation products from numerical weather prediction models – here, the ERA-Interim data record, see Dee et al, 2011 and http://www.ecmwf.int/research/era/do/get/era-interim).

Highlights

- Cloud screening makes optimal use of the multi-channel information from SEVIRI.

- Different tests are applied: surface type (land, sea), solar illumination (daytime, nighttime, twilight, sunglint), and viewing angles are criteria for the application of a certain test.

- Daytime conditions with good illumination (i.e, conditions enabling access to information in all spectral channels) provide best cloud screening results.

- Transition between day- and night-time is smoothed with the temporal dependence twilight test (Derrien and Le Gléau, 2010).

Limitations

- Not all clouds will be detected due to inherent limitations of the SEVIRI imager as being a passive radiometer with a rather coarse field of view (3 x 3 km² at sub-satellite point). This can be compared to actively probing instruments (like cloud lidars and radars) with a much higher cloud detection sensitivity.

- Some thin clouds (particularly, ice clouds) over cold ground surfaces may remain undetected, especially during nighttime, even if having cloud optical thicknesses higher than the above mentioned detection limit.

- The cloud detection algorithm changes from VIS/IR to an infrared only version at the transition from day to night. Even though we applied the SAF NWC MSG v2012 package with a special twilight transition procedure, the switch from day- to night-time algorithm remains present. Irregularities can occur as spikes in the diurnal cycle.

- Since SEVIRI is mounted on geostationary satellites, the well-known dependency of retrieved cloud cover on viewing zenith angle (e.g., Maddux et al., 2010) leads to an overestimation of cloudiness towards the edge of the disc.

Validation

CLAAS-2 CFC was validated in detail with a number of independent data sets in [RD 1]. The results can be summed up as follows. In comparison with manual SYNOP observations, performed mainly over densely populated land areas in the SEVIRI disc (e.g., Europe), CLAAS-2 CFC is on average about 4% (absolute value) higher. CFC was also evaluated against the recently produced collection 6 data from the comparable instrument MODIS which is considered to be the most advanced and best explored passive sensor in space. Averaged over the SEVIRI disc, the differences in CFC are very small, CLAAS-2 being about 1% lower.

Near the SEVIRI sub-satellite point MODIS CFC tends to be higher than CLAAS-2, while the opposite is true towards the edge of the disc. This feature was also found in the comparisons with SYNOP data, and is consistent with the expectation that retrieved cloud cover increases with viewing angle.

Finally, the cloud mask was compared with the space-based lidar instrument CALIOP. The probability of detecting of a cloud was found to be 87%, while the false alarm ratio was 17%. Surprisingly, the long-term disc average CFC from CLAAS-2 was found to be slightly higher than that from CALIOP, even without filtering of the CALIOP data for very thin clouds. This finding needs to be further investigated and may be related to low broken clouds being partly absent in the specific CALIOP dataset used.

All long-term comparisons indicate that CLAAS-2 CFC is very stable over time (see for example the comparison with MODIS in Figure 5-2), showing no discontinuities with changes between the MSG satellites.

Overall, the CLAAS-2 level-2 cloud mask fulfils the threshold requirements compared with CALIOP, while the level-3 CFC product fulfils the optimal requirements (bias less than 5%) with respect to SYNOP and MODIS.
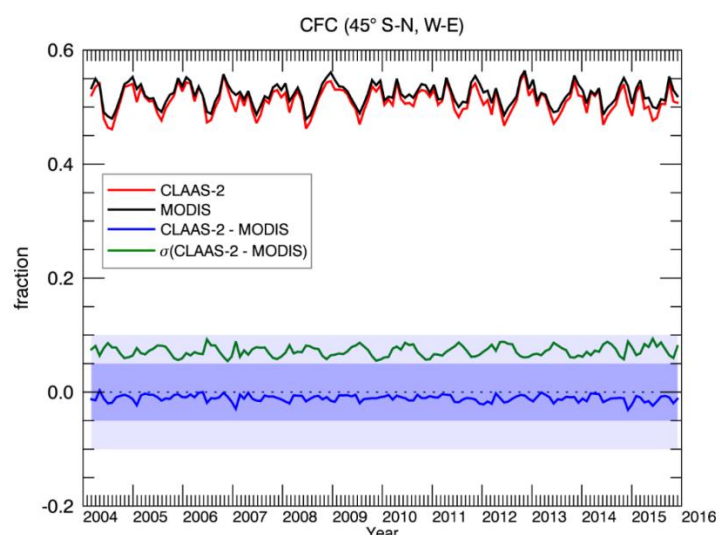
Figure 5-2: Time series of the 45° W-E and S-N area-averaged cloud fractional cover from CLAAS-2 and Aqua MODIS, their biases and the corresponding standard deviations. Optimal and target bias zones are indicated by dark and pale shading, respectively. The optimal standard deviation of the bias is 0.1 (=10%).

Recommended applications

The product can be used without restriction, although users should keep in mind that CFC is overestimated at high viewing angles, i.e. towards the edge of the SEVIRI disc. Possible applications of cloud fractional cover are all those which require stable multi-annual and/or spatiotemporally highly resolved CFC values. Tracking of convective cloud systems like thunderstorm fields (Goyens *et al.*, 2011) or monitoring convective initiation in middle Europe (Siewert *et al.*, 2010) shall serve as an example here. The CFC product is also suitable for the evaluation of regional climate model simulations. As an example, Pfeifroth et al. (2012) evaluated the diurnal cycle of cloud cover in the COSMO-CLM regional climate model using CLAAS-1 data.

5.2   Cloud Top level – CTO

CTP CLAAS-2, 2004/02-2015/12
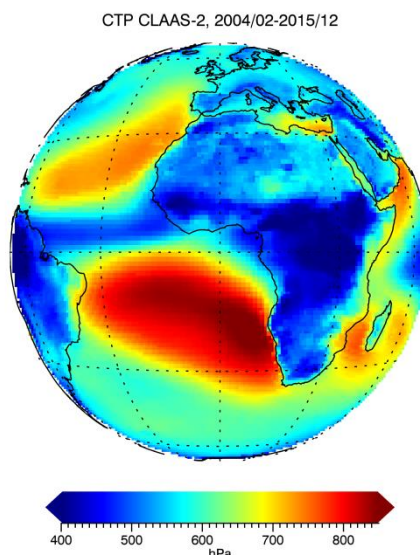
Figure 5-3: CLAAS-2 cloud top pressure averaged from 02/2004 to 12/2015 monthly means.

Three versions of the CLAAS Cloud Top product exist:

1. The Cloud Top Temperature (CTT), expressed in Kelvin
2. The Cloud Top Height (CTH), expressed as height (m) above sea level
3. The Cloud Top Pressure (CTP), expressed in pressure co-ordinates (hPa)

Daily and monthly average products are calculated by averaging the original algorithm output in SEVIRI pixel resolution for all available scenes. All products are averaged arithmetically (linearly) but for the CTP product also a geometric mean (i.e., average of the logarithm of cloud top pressure) is available. As an example, the multi-year mean CTP is presented in Figure 5-3.

Short Algorithm description

For the determination of cloud top information, the NWC SAF algorithms are used, details can be found in [RD 1]. The algorithm is applied to all cloudy pixels as identified by the SAF NWC MSG v2012 cloud mask product.

In a first step, cloudy pixels are separated into three classes depending on cloud type or its opacity respectively: 1) very low, low or medium thick as well as middle level clouds, 2) high opaque clouds and 3) high semi-transparent clouds.

Using RTTOV (http://research.metoffice.gov.uk/research/interproj/nwpsaf/rtm/) the corresponding radiances and brightness temperatures for overcast and clear sky are simulated for each pixel, with vertical profiles of temperature and humidity analysis from ERA-Interim (Dee et al., 2012) as ancillary input. The SEVIRI channels used are: 6.2, 7.3, 13.4 10.8, 12.0 μm.

For very low, low or medium thick clouds as well as opaque clouds the cloud top pressure is retrieved as the best fit between the simulated and the measured 10.8 μm brightness

temperatures. Also the possibility of a low level thermal inversion is taken into account with the help of the ERA-Interim temperature profile at the respective pixel. In that case the very low, low or medium clouds are assumed to form at the inversion level, while they can also rise above that level if their brightness temperatures are colder than the air temperature below the thermal inversion. The type of the inversion (dry air above the inversion level or not) is included by subtracting a variable offset.

In case of semitransparent clouds, the radiance rationing method is used, in which the ratio of radiances from 2 channels is compared to simulated radiances at clear sky conditions for a fixed temperature profile or H2O/IRW intercept method. For the latter a linear relationship of radiance between 2 spectral bands is assumed, but a curve for a window and a sounding channel. For opaque clouds this technique is always applied as preceding test, in order to remove any pixels that are semitransparent but were in fact falsely labeled as opaque by the cloud type test.

Highlights

- Cloud top heights are determined using the reference profiles available from the ERA-Interim data record. The ERA-interim fields have been spatially remapped to a pre-defined grid covering the SEVIRI disc. During run time, the vertical profiles used are temporally interpolated to the exact slot time using the two nearest in time spatially remapped ERA-Interim fields.

- In case of a thermal inversion in the ancillary NWP fields, the clouds are usually positioned at this inversion. However, very low, low or medium clouds can also rise above the inversion level if their brightness temperatures are colder than the air temperature below the thermal inversion. The method accounts also for the atmospheric state above the inversion level (dry air above the inversion level or not).

- In case the cloud top level algorithm has not converged for a particular pixel, the cloud top level of a nearby pixel is inserted. Thus, every pixel masked as cloudy is assigned cloud top level values, which then enables the retrieval of cloud optical and microphysical properties.

Limitations

- Infrared radiation observed by a passive sensor emanates from a certain optical depth within the cloud. In the case of clouds which are optically thin in the upper layers (notably high ice clouds), this typically causes an underestimation of the cloud top height that may amount to several kilometers (e.g., Hamann et al., 2014).

- Clouds are multi-layered in at least 20% of the cases on a global scale. For multi-layered cloud situations, only the top height of the uppermost layer is retrieved. In addition, lower cloud layers usually lead to a negative bias in the retrieval of CTH of the uppermost layer (Hamann et al., 2014).

- The quality of the CTO product depends to some extent on the quality of the reference vertical profiles of temperature and moisture taken from NWP model analyses. Especially troublesome is the treatment of situations with temperature inversions since this implies that there are several solutions to the problem of matching measured cloud

top temperatures to vertical reference profiles. Details of the impact of varying NWP information on CTO products are included in the visiting scientist study from Trolez et al. (2008). Also a direct comparison of the influence of ERA Interim input compared to GME input for the SEVIRI cloud top retrieval was undertaken in Fuchs (2012).

- Cloud top pressure is erroneous if clouds were assigned a wrong type, this results for example in an underestimation of cloud top height/pressure for semi-transparent clouds classified as low/medium or an over estimation of cloud top height/pressure for low/medium clouds classified as semi-transparent

Validation

CLAAS CTO was validated with CALIOP (level-2) and compared with MODIS (level-3) observations.

The validation with CALIOP was performed with and without filtering thin upper cloud layers. The validation showed best agreement when the filtering was applied down to an integrated optical depth of around 0.2 (see Figure 5-4). In that case the bias for CLAAS-2 CTH was -520 m, while and CTP was nearly unbiased, thus fulfilling the target requirements. Without filtering larger differences were obtained.
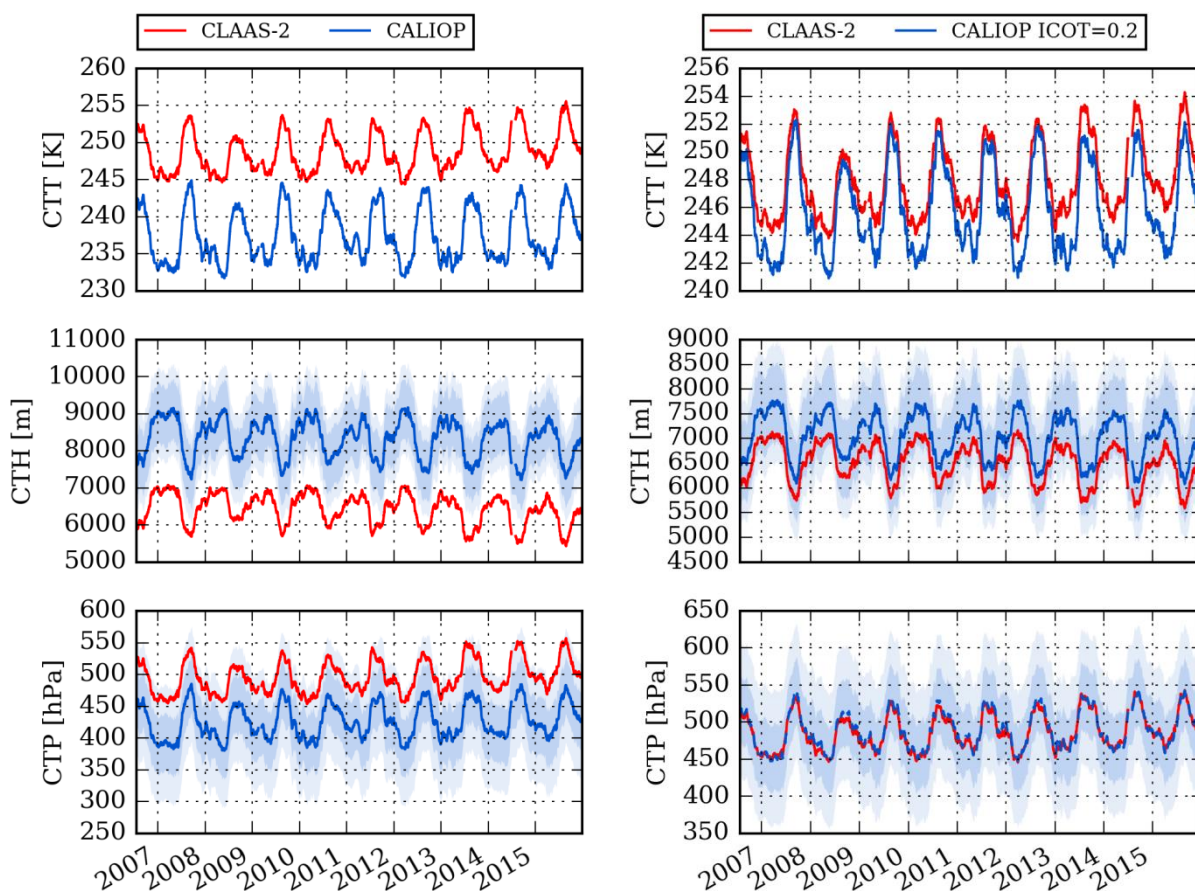
Figure 5-4: Ten-day moving average of cloud top products. In the left panel we compare against the uppermost CALIOP cloud layer, in the right panel we compare against the CALIOP cloud layer where ICOT exceeds the 0.2 threshold. The red curve (CLAAS-2) is identical in both plots. Darker and lighter blue shadings

indicate the target and threshold requirements, respectively. For better visibility, only every 100th matchup is plotted here.

The comparisons with MODIS indicated that the average CTH was higher and CTP lower for CLAAS-2 than for MODIS, albeit with regional differences. The optimal accuracy was reached for CTH, whereas for CTP – which turns out to have somewhat stricter requirements – the threshold was fulfilled.

The time series of CTO are generally stable, but a slight decrease / negative trend in CTH (and positive trend in CTP) is noticed both in comparison with CALIOP and with MODIS, the causes of which are currently not understood.

Recommended applications

For CTO, similar recommendations as for the CFC products (see above) are given, including the applicability at high viewing zenith angles. Possible applications of CTO are all those which require stable, multi-annual, and/or spatiotemporally highly resolved CTO values. It is possible for example to study the travelling of the inter tropical convergence zone (ITCZ) throughout the years or facilitate research on transition from one cloud development stage to another, such as the transition from stratocumulus to cumulus. The product can also used for the evaluation of regional climate model simulations. As an example, Kuell and Bott (2009) used SEVIRI-derived cloud-top pressure to evaluate a convection parameterization scheme in the COSMO model.

5.3   Cloud Phase – CPH

Short Algorithm description

CPH CLAAS-2, 2004/02-2015/12
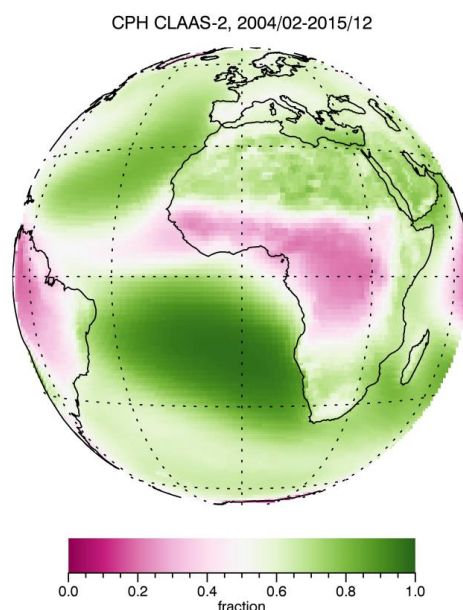
Figure 5-5: CLAAS-2 liquid cloud fraction averaged from 02/2004 to 12/2015 monthly means.

The cloud phase product is meant to represent the thermodynamic phase of the particles near the cloud top. The cloud-top phase retrieval follows the PATMOS-x algorithm (Heidinger et al., 2013), and is based on a number of threshold tests using SEVIRI channels IR_3.9, IR_6.2, IR_8.7, IR_10.8, IR_12.0, and IR_13.4. Some of the tests involve clear and cloudy-overcast radiances, which are calculated using RTTOV. The algorithm is run for cloudy pixels and initially yields one of the following cloud types: liquid, supercooled, opaque ice, cirrus, overlap, and overshooting. These are then further condensed to liquid (former two) and ice (latter four) phase. Details on the algorithm can be found in [RD 4]. For an example of the cloud phase see Figure 5-5.

Highlights

- The algorithm provides cloud phase both during daytime and nighttime.

- In addition to liquid/ice discrimination a further breakdown into cloud types is provided.

- The phase discrimination shows good agreement with active CALIOP observations.

Limitations

The main limitations of the CPH retrieval are:

- The identification of thin cirrus over water clouds is challenging.

- Due to the nature of passive satellite observations, the phase near the top of the clouds is retrieved with limited sensitivity to lower cloud layers.

Validation

Thermodynamic phase is evaluated in [RD 1] in terms of the fraction of liquid clouds relative to the total cloud fraction.

The CLAAS-2 CPH product shows excellent agreement with CALIOP, with hardly any bias, if the CALIOP phase is taken at an optical depth of 0.2 from above into the cloud. If this filtering is not applied, CLAAS-2 has a much larger fraction of liquid clouds than CALIOP.

CPH level-3 was also compared with MODIS. The multi-year mean liquid cloud fraction is compared with Aqua MODIS in Figure 5-6. The MODIS Infrared (IR) cloud phase product is used here, for consistency purposes, while Terra MODIS data are excluded from this analysis due to a calibration degradation issue. The CLAAS-2 phase agrees very well with the MODIS product. On average, the bias of CLAAS-2 phase against MODIS is small and easily within the optimal requirement of 5%. The bc-RMS is around 10%, which is the optimal requirement.

There are hints for a small positive trend in CLAAS-2 liquid cloud fraction in the latest ~3 years of the data record.
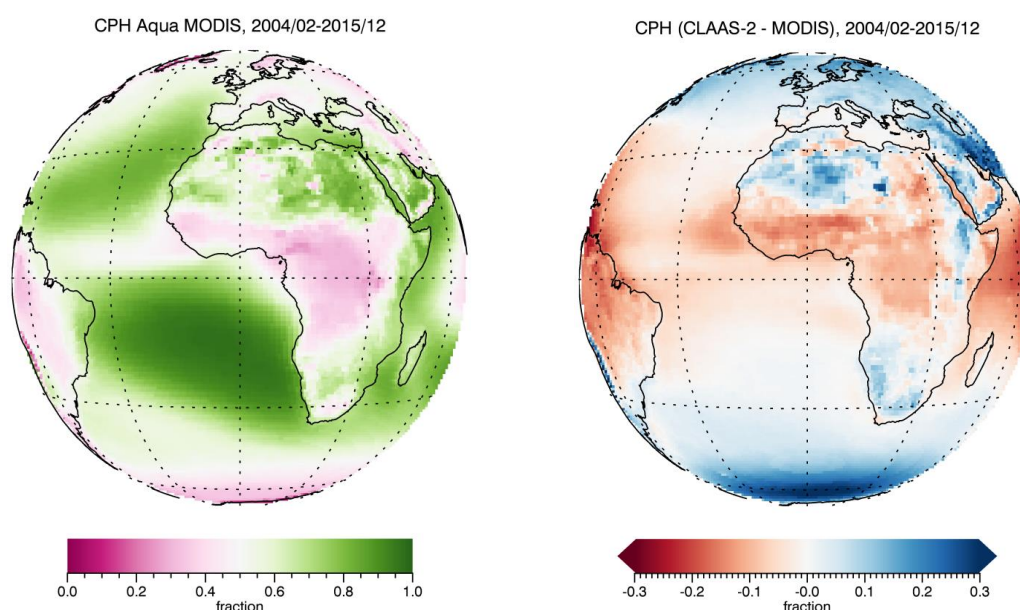
Figure 5-6: Difference between CLAAS-2 and MODIS fraction of liquid clouds (relative to total cloud fraction) averaged from 02/2004 until 12/2015.

Recommended applications

The CPH data record is specifically useful for studies of cloud development, e.g. convective activity characterized by a transition from liquid to ice phase as the clouds grow vertically. In general, wherever multi annual, stable and spatiotemporally highly resolved information is needed, CPH data from SEVIRI can be applied. Analysis of the detection of Cd/Tcu clouds is mentioned here as an example (Carbajal Henken et al., 2011).

5.4   Liquid Water Path – LWP

Short Algorithm description

The central principle of the method to retrieve cloud optical and microphysical properties is that the reflectance of clouds at a (for cloud particles) non-absorbing wavelength in the visible region (e.g., 0.6 or 0.8 μm) is strongly related to the optical thickness (τ) and has little dependence on particle effective radius (r_e), whereas the reflectance of clouds at an absorbing wavelength in the shortwave-infrared region (e.g., 1.6 or 3.7 μm) is strongly dependent on effective radius (Nakajima and King, 1992).

In the CPP algorithm (Roebeling et al. 2006), the Doubling-Adding KNMI (DAK) radiative transfer model (De Haan et al. 1987 and Stammes 2001) is used to simulate 0.6- and 1.6-μm top-of-atmosphere reflectances of homogeneous, plane-parallel clouds as a function of viewing geometry, cloud optical thickness, effective radius, and cloud phase. These simulated reflectances are stored in a look-up table (LUT).

τ and r_e are retrieved for cloudy pixels in an iterative manner by matching satellite-observed reflectances to the LUT of RTM-simulated reflectances. From these two properties, the cloud water path (CWP) of water clouds (or liquid water path, LWP) can be computed using the following relation (Stephens, 1978):

$$CWP = 2/3 \; \rho_l \; \tau \; r_{e,}$$

where ρ_l is the density of liquid water. For water clouds effective radii between 3 and 34 μm are retrieved.

CLAAS-2 all-sky LWP, 2004/02-2015/12

Figure 5-7: CLAAS-2 all-sky liquid water path averaged from 02/2004 to 12/2015 monthly means.

Highlights

- Together with LWP, τ and r_e are included as additional layers in the level-2 and level-3 products.

- An estimate of the LWP retrieval error is reported.

- The careful calibration of the shortwave SEVIRI channels with MODIS (Meirink et al., 2013) has a pronounced effect on the quality of the retrieved τ and r_e, and thus LWP.

- The effect of absorption by trace gases in the atmosphere on shortwave narrowband reflectances is taken into account using MODTRAN (Berk et al. 2000) simulations (Meirink et al. 2009).

Limitations

The main limitations of the LWP retrieval are:

- The derivation of cloud physical properties from reflected solar radiation is dependent on the availability of daylight. This means that no retrievals can be done during night time. Even if pixel-level retrievals are performed and reported up to solar zenith angles of 84°, for level-3 aggregation a maximum solar zenith angle of 75° is applied. Similarly, the retrievals become less accurate at very high viewing angles, i.e. near the edge of the disc.
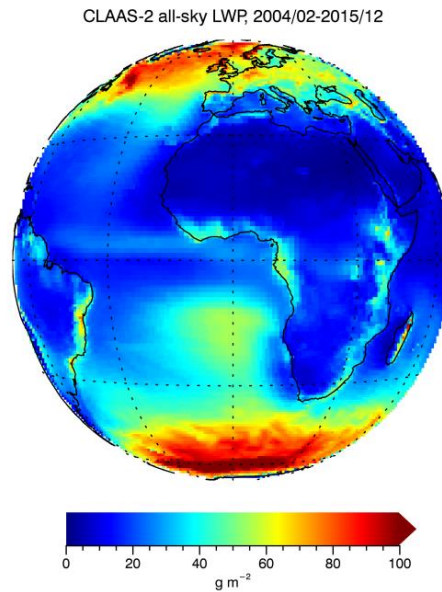
- The retrieval is highly problematic over very bright surfaces, particularly ice and snow, as the visible reflectance from clouds is similar to that from the surface.

- Cloud property retrievals are performed assuming that clouds are plane parallel. Two prominent examples of cases for which this assumption is violated are: (1) three-dimensional radiative effects become important if large sub-pixel variations in cloud-top height occur, and particularly if the solar zenith angle is large; (2) retrievals for broken clouds are affected by a reflectance contribution from the surface.

- Aerosols are not considered in the CPP retrieval. This assumption is usually justified because aerosols reside below or within the cloud and their optical thickness is small compared to that of the cloud. However, if the aerosols reside above the cloud and if they are sufficiently absorbing, they can significantly lower the visible reflectance. This leads to underestimations of both τ and r_e, and thus LWP (Haywood et al. 2004).

- Unlike active satellite instruments, which can derive cloud profile information, retrievals from passive satellite instruments are limited by the fact that the obtained signal emanates from the integrated profile. Since near-infrared radiation is only penetrating into the cloud to a certain depth (due to absorption by cloud particles), the retrieved effective radius is representative for the upper part of the cloud (Platnick 2001). The penetration depth depends on the amount of absorption by cloud particles, which is increasing with wavelength. This means that the retrieved CPH and r_e depend on which NIR spectral channel is used (in our case 1.6 μm).

- Because the retrieval of effective radius becomes unreliable for thin clouds, weighting with a climatological average r_e is performed for clouds with $\tau < 5$. Although this stabilizes the retrieval results, it does not take away the inherent uncertainty in r_e retrievals for thin clouds.

Validation

The CLAAS-2 LWP product is evaluated in [RD 1] with passive microwave observations (level-2 AMSR-E data and the UWisc level-3 dataset) as well as with MODIS. The comparisons with UWisc focus on a region in the south Atlantic dominated by stratocumulus fields. For this region, CLAAS-2 LWP is on average consistent with the microwave based data, although the seasonal variability is smaller.

The comparison with MODIS is illustrated in Figure 5-8 showing that LWP spatial distributions agree well. Specific regions with high LWP along parts of the west coast of Africa and near the polar regions can be consistently observed in both datasets. CLAAS-2 all-sky LWP is relatively smaller than MODIS over land and larger over ocean. The CLAAS-2 and MODIS time series are in very good agreement, with overall slightly higher CLAAS-2 values and an identical seasonal cycle. The bias is within the optimal requirement of 5 g m^{-2}, and the bc-RMS is also within the 10 g m^{-2} optimal threshold.

Figure 5-8: MODIS all-sky liquid water path (left) and its difference with CLAAS-2 (right) averaged from 02/2004 until 12/2015.

Recommended applications

The LWP data record is most reliable at lower latitudes, or (better said) lower solar zenith angles (below about 65 degrees). In addition, high latitudes are frequently affected by snow and ice cover. In these cases retrievals are problematic, even more because our ancillary database currently does not represent snow and ice cover well. Also, the viewing angle of SEVIRI should be small enough, to inhibit cloud geometry errors.

In general, use of LWP is feasible where multi annual, stable and spatiotemporally highly resolved information is needed. Model evaluation of (the diurnal cycle of) cloud water path is one of the possible applications, see e.g., Roebeling and van Meijgaard (2009) and Greuell et al. (2011).

5.5   Ice Water Path – IWP

Short Algorithm description

Ice water path is retrieved in te same way as LWP but with τ and r_e retrievals based on RTM simulations for imperfect hexagonal ice crystals. Homogeneous distributions of ice crystals from the COP library (Hess et al., 1998) are assumed, with effective radii ranging between 5 and 80 µm. The multi-annual mean IWP is shown in Figure 5-9.
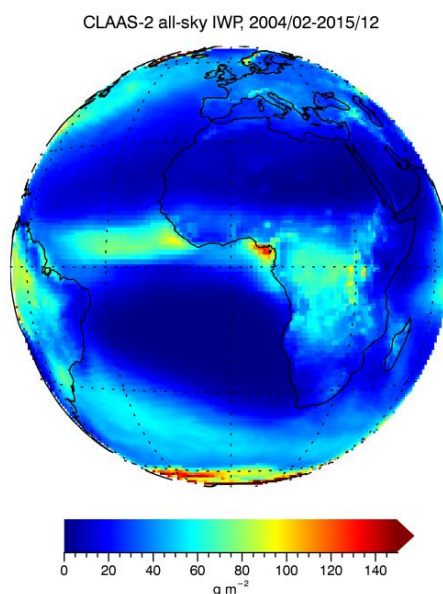
Figure 5-9: CLAAS-2 all-sky ice water path averaged from 02/2004 to 12/2015 monthly means.

Highlights

- The use of imperfect hexagonal ice crystals gives adequate simulations of total and polarized reflectance of ice clouds (Knap et al. 2005).

- An estimate of the IWP retrieval error is reported.

Limitations

The same limitations as for LWP hold also for IWP. In addition, the r_e retrieval for ice clouds is considerably more uncertain than for water clouds, because particle shapes and roughness vary widely and are not well known. The assumptions on ice crystal habits used to generate the LUTs (in our case imperfect hexagons are assumed) have a profound impact on the retrieved r_e and IWP.

Validation

The CLAAS-2 IWP product is evaluated in [RD 1] with DARDAR observations for level-2 as well as with MODIS for level-3. Compared with DARDAR, the CLAAS-2 IWP is overall negatively biased, especially for the thicker clouds. This bias mainly originates from the effective radius, which is considerably smaller in CLAAS-2 than in DARDAR (a weighted

average of the profile near the cloud top was used as a reference), and shows no correlation. Comparisons with MODIS also indicate that the CLAAS-2 ice REFF is rather small.

Multi-year mean spatial distributions and area-averaged time series of CLAAS-2 all-sky IWP were compared with MODIS. As for LWP there is a remarkable agreement in the spatial patterns, especially along the ITCZ, see Figure 5-10. CLAAS-2 IWP is overall somewhat lower than MODIS IWP. An exception is the southern Atlantic near Antarctica, a region that is seasonally covered with sea ice, over which CLAAS-2 likely overestimates IWP, while MODIS – with its many additional channels – allows more accurate retrievals.

The seasonal cycles of CLAAS and MODIS IWP agree very well, with overall slightly lower CLAAS-2 values, and the bias is within the optimal requirement of 10 g m^{-2}, while the bc-rms also reaches the optimal requirement of 20 g m^{-2} (see [RD 1]).
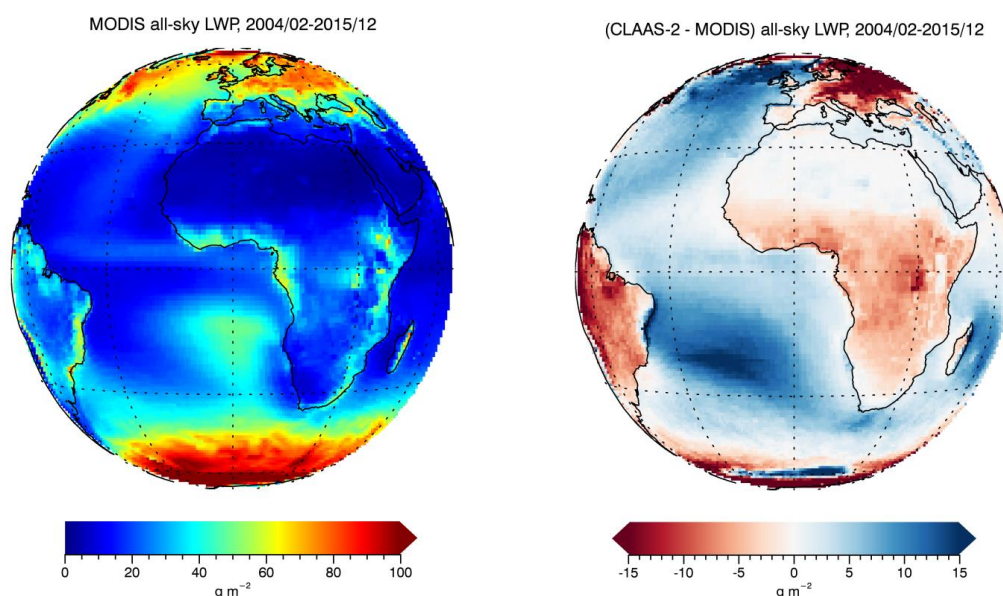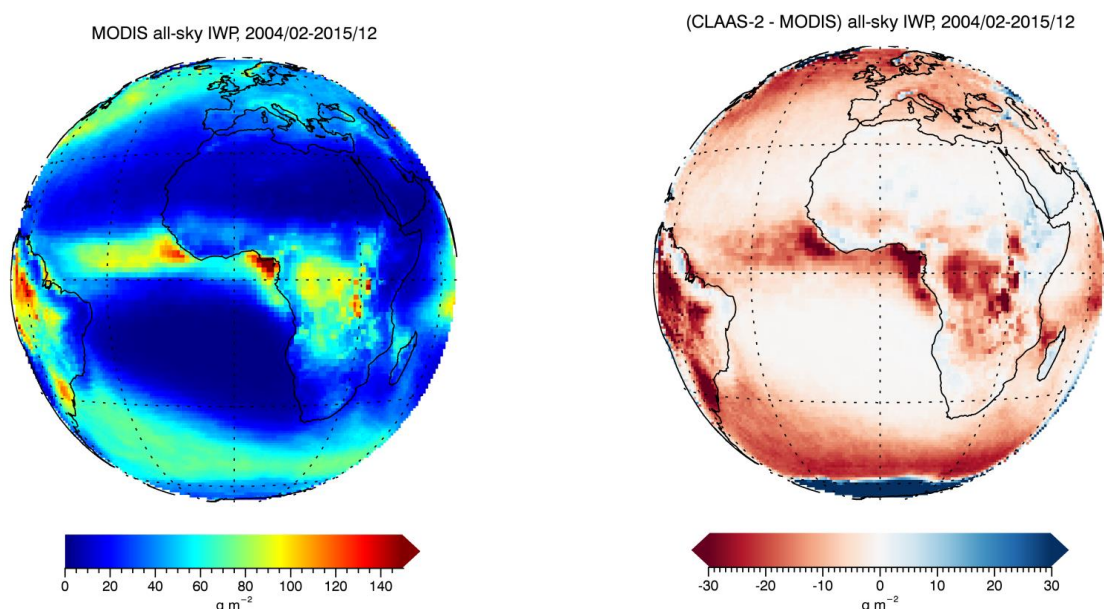

Figure 5-10: MODIS all-sky ice water path (left) and its difference with CLAAS-2 (right) averaged from 02/2004 until 12/2015.

Recommended applications

The IWP data record is just like LWP most reliable at lower latitudes, or lower solar zenith angles below about 65 degrees. In addition, high latitudes are frequently affected by snow and ice cover. In these cases, retrievals are problematic, even if our ancillary database does include snow and ice cover to allow a better estimate of surface albedo. Also, the viewing angle of SEVIRI should be small enough, to inhibit cloud geometry errors.

IWP can like LWP be applied where multi annual, stable and spatiotemporally highly resolved information is needed. Model evaluation of the diurnal cycle of cloud water path is one of the possible applications, see Roebeling and van Meijgaard (2009).

5.6   Joint Cloud property Histogram – JCH
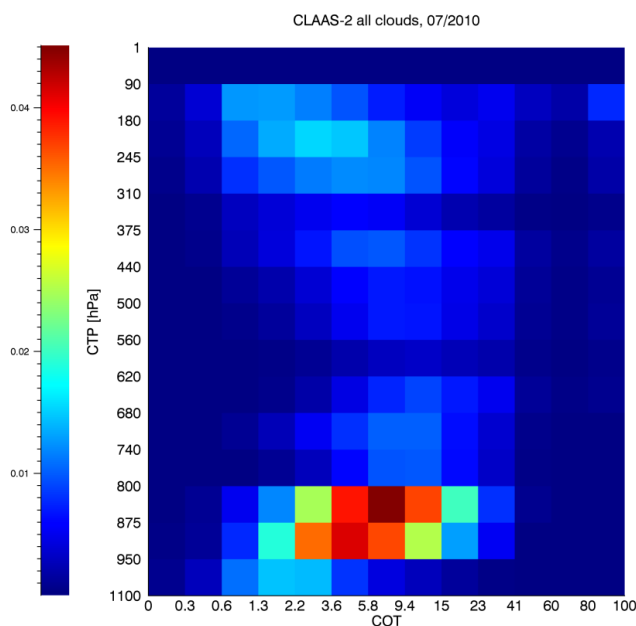
Figure 5-11: JCH, a 2D histogram of cloud top pressure and cloud optical thickness, here aggregated over the 45° S-N, W-E area for 07/2010.

Short Algorithm description

The JCH product is a combined histogram of CTP and COT covering the solution space of both parameters. This two-dimensional histogram gives the absolute numbers of occurrences for specific COT and CTP combinations defined by specific bins. It is further separated in liquid and ice clouds. An example of JCH for July 2010 is shown in Figure 5-11.

Highlights

- The product adds value to the single standard Level 3 products of CTP and COT by showing how the two parameters vary together.

- The histograms are given for each grid point which means that a user can aggregate results over any local or regional domain in order to analyse typical cloud regimes (or types).

- The use of joint histograms is common in applications for evaluating climate models.

- The CLAAS-2 COT and CTP bins for the JCH product have been chosen such that they are a superset of the traditional ISCCP bins. Thus, the CLAAS-2 product can be aggregated to exactly the same bins as used for the ISCCP product.

Limitations

- The product is only available during daytime since the COT parameter is not retrieved at night

Recommended applications

With the JCH diagrams the discrimination between different cloud regimes is supported. COT and CTP information can readily be considered in a more statistical way. Since the CM SAF JCH product is compiled as distributions for each grid point, it is possible to compose cloud distribution statistics for any region size on the globe by simple aggregation of grid point values. As an example, the CLAAS-1 JCH was used by Van Weverberg et al. (2012) to evaluate model-simulated cloud properties.

6 Summary table of validation results regarding product accuracy

Table 6-1 shows the achieved accuracies of the cloud products as discussed in [RD 1]. The acronyms used are: SYNOP = Synoptical surface observations, CALIOP = Cloud-Aerosol Lidar with Orthogonal Polarisation, MODIS = Moderate Resolution Imaging Spectroradiometer, and UWisc = University of Wisconsin passive microwave based LWP dataset. All references are described in detail in [RD 1].

Table 6-1: Summary of CLAAS-2 validation results compared to target **accuracy** requirements for each cloud product. The accuracies are formulated in terms of biases. Results from consistency checks / inter-comparisons (using MODIS data, which, due to the sampling, cannot be seen as absolute reference) are marked in **blue**.

Product		**Accuracy requirement** (bias)	**Achieved accuracies**
Cloud Fractional Cover	**(CFC)**	10%	3.8 % (SYNOP) -1.1 % (MODIS)
Cloud Top Height	**(CTH)**	800 m	307 m (MODIS) -520 m (CALIOP)
Cloud Top Pressure	**(CTP)**	45 hPa	-58.6 hPa (MODIS) -2.2 hPa (CALIOP)
Cloud Phase	**(CPH)**	10%	1% (MODIS)
Liquid Water Path	**(LWP)**	10 g m^{-2}	6.17 g m^{-2} (UWisc) 2.05 g m^{-2} (MODIS)
Ice Water Path	**(IWP)**	20 g m^{-2}	-5.11 g m^{-2} (MODIS)
Joint Cloud Histogram	**(JCH)**	n/a	n/a

7 Outlook

The present CLAAS-2 data record is the first complete processing of the SEVIRI time series from 2004 to 2015 by CM SAF. In CDOP 3 (the next phase of the CM SAF project) a follow-up version of the SEVIRI data record will be processed. The experience that we gained while creating and evaluating the current edition will be incorporated into the next data record version.

Some new features will be:

- The applied algorithms will be updated after a careful testing of performance and quality.

- The possibility of including more error characteristics of the processed variables will be explored.

- The length of the data record will be increased.

- The calibration will be extended re-assessed using findings from the Global Space-Based Inter-Calibration System (GSICS) project, in particular for the infrared channels.

Finally, developments towards integrating the new series of EUMETSAT geostationary satellites – Meteosat Third Generation (MTG) carrying the Flexible Combined Imager (FCI) – will start.

The Calipso and CloudSat datasets were found to deliver very valuable information for the analysis of CLAAS-2 at Level 2 stage. This role will be taken over by the EarthCARE mission, which is currently planned to be launched in 2018.

8 Data format description

CLAAS-2 products are provided as NetCDF-4 (Network Common Data Format v4) files (http://www.unidata.ucar.edu/software/netcdf/) with internal compression. The data files are created following NetCDF Climate and Forecast (CF) Metadata Convention version 1.6 (http://cf-pcmdi.llnl.gov/) and NetCDF Attribute Convention for Dataset Discovery version 1.3.

For data processing and conversion to various graphical packages input format, CM SAF recommends the usage of the climate data operators (CDO), available under GNU Public License (GPL) from MPI-M (http://www.mpimet.mpg.de/~cdo).

8.1 Data format description of non-averaged products

Level 2 data are stored in the native satellite projection. The corresponding lat-lon grid is available in a separate auxiliary file, see Section 8.2.4.

8.2 General variables

CLAAS-2 L2 data are provided on a grid of 3636 x 3636 pixels, excluding a number of space pixels at the edge of the SEVIRI full disk. In all product files the same set of general variables are used:

time   observation timestamp in days since 1970-01-01 00:00 UTC

time_bnds   two-dimensional array reporting the actual temporal coverage of the observation for each timestamp in variable *time*

8.2.1 Attributes

The data fields provide a set of general attributes, which are listed and described in Table 8-1. Bold attributes are mandatory for each non-coordinate variable. If available, a standard_name is provided..

Table 8-1: Common attributes of each variable in level 2 data.

Name	Description
_FillValue	*This number represents missing or undefined data. Missing values are to be filtered before applying scale factor and offset*
valid_range	*Specifies the valid range of the data [min,max]*
long_name	*Long descriptive name of the variable*
standard_name	*Standard name that references a description of a variable's content in the CF standard name table*
scale_factor	*The data are to be multiplied by this factor after it is read*
add_offset	*This number is to be added to the data after it is read. If scale_factor is present, it has to be applied first.*
units	*Physical unit*
flag_values, flag_masks, flag_meanings	*These attributes describe variables containing status flags. The flag_values/flag_masks attributes describe all possible values of the status flag, whereas flag_meanings indicates the meaning of a certain*

flag value. See section 3.5 in the CF standard for details.

If *scale_factor* or *add_offset* are present, the data have been scaled. To obtain the physical value *y* of a variable *x*, multiply it by *scale_factor* and add *add_offset* afterwards:

$$y = scale\_factor*x + add\_offset$$

8.2.2 Product specific data fields

This section provides a detailed description of each variable in the CLAAS-2 level 2 products. Please note that we use the FORTRAN-like dimension order here. The *ncdump* utility for example, displays the dimensions in reversed (C-like) order.

Cloud mask
> *cma(x, y, time)*
>> field contains the binary cloud mask
> *cma_quality(x, y, time)*
>> field contains the cloud mask quality flag
> *cma_test(x, y, time)*
>> field contains the cloud mask retrieval test that detects a cloud first

Cloud top
> *ctt(x, y, time)*
>> field contains the cloud top temperature
> *ctp(x, y, time)*
>> field contains the cloud top pressure
> *cth(x, y, time)*
>> field contains the cloud top height
> *interpolation(x, y, time)*
>> specifies whether cloud top values in a certain pixel have been obtained by interpolation ([RD 2], [RD3])
> *quality(x, y, time)*
>> field contains the retrieval flag

Cloud physical properties
> *ct(x, y, time)*
>> field contains the cloud type
> *cph(x, y, time)*
>> field contains the cloud phase
> *cwp(x, y, time)*
>> field contains the cloud water path (LWP or IWP)
> *cot(x, y, time)*
>> field contains the cloud optical thickness
> *reff(x, y, time)*
>> field contains the droplet / ice particle effective radius
> *cwp_error(x, y, time)*

field contains the retrieval error in CWP

cot_error (x, y, time)

field contains the retrieval error in COT

reff_error(x, y, time)

field contains the retrieval error in REFF

h_sigma(x, y, time)

field contains the relative standard deviation of the visible reflectances

quality(x, y, time)

field contains the retrieval quality flag

8.2.3 General attributes

Each level 2 NetCDF file also possesses general attributes that are valid for all variables contained in this file. These attributes are described in Table 8-2.

Table 8-2: General attributes of a non-averaged NetCDF file.

Name	Description
comment	*Data in this file are stored in SEVIRI image coordinates. Please visit the DOI page to obtain the corresponding Lat-Lon grid.*
id	*DOI:10.5676/EUM_SAF_CM/CLAAS/V002*
product_version	*2.0*
creator_name	*DE/DWD*
creator_email	*contact.cmsaf@dwd.de*
creator_url	*http://www.cmsaf.eu*
institution	*EUMETSAT/CMSAF*
project	*Satellite Application Facility on Climate Monitoring (CM SAF)*
references	*http://dx.doi.org/10.5676/EUM_SAF_CM/CLAAS/V002*
platform	*Earth Observation Satellites > METEOSAT > METEOSAT-8 (or 9 or 10)*
instrument	*Earth Remote Sensing Instruments>Passive Remote Sensing >Spectrometers/Radiometers>Imaging Spectrometers/Radiometers>SEVIRI>Spinning Enhanced Visible and Infrared Imager*
time_coverage_start	*Temporal coverage start of the data [ISO8601 date]*
time_coverage_end	*Temporal coverage end of the data [ISO8601 date]*
time_coverage_duration	*Temporal coverage duration of the data [ISO8601 date]*
geospatial_lat_min	*-81.2*
geospatial_lat_max	*81.2*
geospatial_lat_units	*degrees_north*
geospatial_lon_min	*-81.26*
geospatial_lon_max	*81.26*
geospatial_lon_units	*degrees_east*
keywords	*EARTH SCIENCE>ATMOSPHERE>CLOUDS>"variable group"*
Conventions	*convention tables for metadata and attributes (CF-1.6, ACDD-1.3)*
keywords_vocabulary	*Vocabulary for keywords in the global attributes (GCMD Science Keywords, Version 8.1)*
standard_name_vocabulary	*Vocabulary for standard names in the parameter attributes (Standard Name Table (v28, 07 January 2015))*
instrument_vocabulary	*Vocabulary for the instrument in the global attributes (GCMD Instruments, Version 8.1)*
platform_vocabulary	*Vocabulary for the platform in the global attributes (GCMD Platforms, Version 8.1)*

Name	Description
date_created	*Point in time, when the file was created [ISO8601 date]*
CMSAF_proj4_params	*Projection parameters for PROJ.4 library*
CMSAF_area_extent	*Projection coordinates of the area corners in meters [lower left x, lower left y, upper right x, upper right y]*
CMSAF_L2_processor	*SAFNWC MSG v2012 with custom CMSAF modifications*
CMSAF_reprocessing_ software	*seviri-v1.0 (<commit hash>)*

8.2.4 Auxiliary data

The CLAAS-2 level 2 data record goes along with a set of auxiliary data. Because the SEVIRI disc and its viewing geometry are (quasi) constant with time, there is no need to include auxiliary information into the product files. Instead, latitude and longitude fields as well as satellite zenith angles for different subsatellite points, land sea mask and altitude are provided in an extra file, which are available via the DOI webpage.

8.3 Monthly and daily mean data file contents

A common NetCDF file consists of dimensions, variables, and attributes. These components can be used together to capture the meaning of data and relations among data. All CLAAS-2 product files are built following the same design principles. The averaged data are provided as daily and monthly means and as mean diurnal cycle. For the latter all time slots within one hour are averaged to a daily mean diurnal cycle. All diurnal cycles of a month are averaged to the monthly mean diurnal cycle. The daily means are based on all available time slots. The monthly mean is an average of all daily means. The product files contain general variables, which are common for all files, and product specific variables. The latter are three-dimensional, except for the histograms. Dimensions of all three-dimensional fields are named *time, lon*, *lat*. For the JCHs, additionally two dimensions for COT and CTP bins are included. All other provided histograms have one additional dimension for variable bins. General variables of each file are *time, time_bnds*, *latitude*, and *longitude* (see section 8.4). All data fields, which are described in section 8.4.2, also contain specific attributes as given in section 8.4.1. Global attributes of each file are reported in section 8.4.3.

8.4 General variables

time
>start of averaging/composite time period; In case of diurnal cycles, this vector has 24 elements
>[days counted from 1970-01-01]

time_bnds
>two-dimensional array defining the averaging/composite time period

lat
>geographical latitude of grid-box centre [degree_north]

lon
>geographical longitude of grid-box centre [degree_east]

8.4.1 Attributes

Table 8-3 summarizes the attributes which are assigned to each data field in the NetCDF files. Keep in mind that, depending on the parameter, some attributes can be omitted, for example if no standard name is defined.

Table 8-3: Attributes assigned to variables in NetCDF.

Name	Description
long_name	*long descriptive name*
standard_name	*standard name that references a description of a variable's content in the CF standard name table*
units	*physical unit*
valid_min	*smallest valid value of a variable*
valid_max	*largest valid value of a variable*
scale_factor	*The data are to be multiplied by this factor after it is read.*
add_offset	*This number is to be added to the data after it is read. If scale_factor is present, the data are first scaled before the offset is added.*
_FillValue	*This number represents missing or undefined data. Missing values are to be filtered before scaling.*

8.4.2 Product specific data fields

This section provides a detailed description of each variable in the CLAAS-2 level 3 products. Please note that we use the FORTRAN-like dimension order here. The *ncdump* utility for example, displays the dimensions in reversed (C-like) order.

8.4.2.1 Fractional cloud coverage (CFC)

nobs(lon, lat, time)
> field containing the number of observations used to create mean CFC
nobs_day(lon, lat, time)
> field containing the number of observations used to create mean daytime CFC
nobs_night(lon, lat, time)
> field containing the number of observations used to create mean nighttime CFC
cfc(lon, lat, time)
> field containing the mean CFC value given in percent
cfc_std(lon, lat, time)
> field containing the standard deviation over all CFC data points
cfc_day(lon, lat, time)
> field containing the mean daytime CFC value given in percent
cfc_night(lon, lat, time)
> field containing the mean nighttime CFC value given in percent
cfc_low(lon, lat, time)
> field containing the mean CFC of all clouds with CTP larger than 680 hPa given in percent
cfc_middle(lon, lat, time)

field containing the mean CFC of all clouds with CTP between 440hPa and 680 hPa given in percent

cfc_high(lon, lat, time)

field containing the mean CFC of all clouds with CTP smaller than 440 hPa given in percent

8.4.2.2   Cloud phase (CPH)

nobs(lon, lat, time)

field containing the number of observations used to create mean CPH

nobs_day(lon, lat, time)

field containing the number of observations used to create mean daytime CPH

cph(lon, lat, time)

field containing the mean liquid cloud fraction given in percent

cph_std(lon, lat, time)

field containing the standard deviation over all CPH data points

cph_dayd(lon, lat, time)

field containing the mean daytime liquid cloud fraction given in percent

cph_day_std(lon, lat, time)

field containing the standard deviation over all daytime CPH data points

8.4.2.3   Cloud top level

nobs(lon, lat, time)

field containing the number of observations used to create mean cloud top products

ctt(lon, lat, time)

field containing the arithmetical mean cloud top temperature (CTT)

ctt_std(lon, lat, time)

field containing the standard deviation over CTT data points

cth(lon, lat, time)

field containing the arithmetical mean cloud top height (CTH)

cth_std(lon, lat, time)

field containing the standard deviation over CTH data points

ctp(lon, lat, time)

field containing the arithmetical mean cloud top pressure (CTP)

ctp_std(lon, lat, time)

field containing the standard deviation over CTP data points

ctp_log(lon, lat, time)

field containing the logarithmic mean CTP

8.4.2.4   Liquid water path (LWP)

nobs(lon, lat, time)

field containing the number of observations used to create mean LWP

SZA(lon, lat, time)

40

field containing the mean solar zenith angle of successful retrieval results and liquid phase results

SZA_std(lon, lat, time)

field containing the standard deviation of the solar zenith angle of successful retrieval results and liquid phase results

lwp(lon, lat, time)

field containing the mean LWP

lwp_allsky(lon, lat, time)

field containing the grid box mean LWP, weighted by the grid box cloud fraction

lwp_std(lon, lat, time)

field containing the standard deviation of the LWP

lwp_error(lon, lat, time)

field containing the mean LWP retrieval error

lwp_std(lon, lat, time)

field containing the standard deviation of the LWP retrieval error

cot_ liq(lon, lat, time)

field containing the mean liquid cloud optical thickness (COT)

cot_liq_std(lon, lat, time)

field containing the standard deviation of the liquid COT

cot_liq_error(lon, lat, time)

field containing the mean retrieval error of the liquid COT

cot_liq_error_std(lon, lat, time)

field containing the standard deviation of the liquid COT retrieval error

cot_liq_log(lon, lat, time)

field containing the logarithmic mean liquid COT

ref_ liq(lon, lat, time)

field containing the mean effective radius of water droplets

ref_liq_std(lon, lat, time)

field containing the standard deviation of the effective radius of water droplets

ref_liq_error(lon, lat, time)

field containing the mean retrieval error of the effective radius of water droplets

ref_liq_error_std(lon, lat, time)

field containing the standard deviation of the effective radius of water droplets retrieval error

8.4.2.5 Ice water path (IWP)

nobs(lon, lat, time)

field containing the number of observations used to create mean IWP

SZA(lon, lat, time)

field containing the mean solar zenith angle of successful retrieval results and ice phase results

SZA_std(lon, lat, time)

field containing the standard deviation of the solar zenith angle of successful retrieval results and ice phase results

iwp(lon, lat, time)

field containing the (cloudy-sky) mean IWP

iwp_allsky(lon, lat, time)

field containing the grid box (or all-sky) mean IWP

iwp_std(lon, lat, time)
> field containing the standard deviation of the IWP

iwp_error(lon, lat, time)
> field containing the mean IWP retrieval error

iwp_std(lon, lat, time)
> field containing the standard deviation of the IWP retrieval error

cot_ice(lon, lat, time)
> field containing the mean ice COT

cot_ice_std(lon, lat, time)
> field containing the standard deviation of the ice COT

cot_ice_error(lon, lat, time)
> field containing the mean retrieval error of the ice COT

cot_ice_error_std(lon, lat, time)
> field containing the standard deviation of the ice cloud COT error

cot_ice_log(lon, lat, time)
> field containing the logarithmic mean ice COT

ref_ice(lon, lat, time)
> field containing the mean effective radius of ice particles

ref_ice_std(lon, lat, time)
> field containing the standard deviation of the effective radius of ice particles

ref_ice_error(lon, lat, time)
> field containing the mean retrieval error of the effective radius of ice particles

ref_ice_error_std(lon, lat, time)
> field containing the standard deviation of the effective radius of ice particles retrieval error

8.4.2.6 Joint Cloud property Histograms (JCH)

hist_phase(hist_phase)
> two-elements vector containing liquid and ice phase

hist2d_cot_bin_border(hist_cot_bin_border)
> vector contains outer limits of the COT bins

hist2d_cot_bin_centre(hist_cot_bin_centre)
> vector contains centre of the COT bins

hist2d_ctp_bin_border(hist_ctp_bin_border)
> vector contains outer limits of the CTP bins

hist2d_ctp_bin_centre(hist_ctp_bin_centre)
> vector contains centre of the CTP bins

cfc(lon, lat, time)
> field containing the mean fractional cloud cover, used to the JCH

hist2d_cot_ctp(lon, lat, hist2d_cot_bin_centre, hist2d_ctp_bin_centre, hist_phase, time)
> field containing the number of occurrences of specific combinations of COT and CTP ranges at given spatial location. The Joint Cloud property Histograms are defined on coarser spatial resolution (0.25°) compared to all other products.

8.4.2.7 One-dimensional histograms

Cloud top histograms

hist_phase(hist_phase)
> two-elements vector containing liquid and ice phase

hist1d_ctt_bin_border(hist_ctt_bin_border)
> vector contains outer limits of the CTT bins

hist1d_ctt_bin_centre(hist_ctt_bin_centre)
> vector contains centre of the CTT bins

hist1d_ctp_bin_border(hist_ctp_bin_border)
> vector contains outer limits of the CTP bins

hist1d_ctp_bin_centre(hist_ctp_bin_centre)
> vector contains centre of the CTP bins

hist1d_ctt(lon, lat, hist1d_ctt_bin_centre,hist_phase,time)
> field contains the number of occurrences of specific CTT ranges at given spatial location.

hist1d_ctp(lon, lat, hist1d_ctp_bin_centre,hist_phase,time)
> field contains the number of occurrences of specific CTP ranges at given spatial location.

Cloud water path histograms (includes LWP and IWP histograms)

hist_phase(hist_phase)
> two-elements vector containing liquid and ice phase

hist1d_cwp_bin_border(hist_cwp_bin_border)
> vector contains outer limits of the cloud water path (CWP) bins

hist1d_cwp_bin_centre(hist_cwp_bin_centre)
> vector contains centre of the CWP bins

hist1d_cot_bin_border(hist_cot_bin_border)
> vector contains outer limits of the cloud optical thickness (COT) bins

hist1d_cot_bin_centre(hist_cot_bin_centre)
> vector contains centre of the COT bins

hist1d_ref_bin_border(hist_ref_bin_border)
> vector contains outer limits of the cloud particle effective radius (REFF) bins

hist1d_ref_bin_centre(hist_ref_bin_centre)
> vector contains centre of the REF bins

hist1d_cwp(lon, lat, hist1d_cwp_bin_centre,hist_phase,time)
> field contains the number of occurrences of specific CWP ranges at given spatial location. Includes IWP and LWP histogram along the *hist_phase* dimension.

hist1d_cot(lon, lat, hist1d_cot_bin_centre,hist_phase,time)
> field contains the number of occurrences of specific COT ranges at given spatial location.

hist1d_ref (lon, lat, hist1d_ref_bin_centre,hist_phase,time)
> field contains the number of occurrences of specific REFF ranges at given spatial location.

8.4.2.8 Mean diurnal cycle

The mean diurnal cycle products are provided as daily mean and monthly mean. They are available for the variables cloud fractional cover, cloud phase, cloud top temperature/pressure/height, liquid/ice water path, liquid/ice optical thickness, effective droplet radius and effective ice particle size. The spatial resolution of the diurnal cycles is 0.25°.

8.4.3 Global attributes

Table 8-4 contains the global attributes of averaged CLAAS-2 L3 final product files. Possible values of the attributes are also given as well as explanations.

Table 8-4: Overview of global attributes of NetCDF files of CLAAS-2 products and possible corresponding values.

Name	Description
title	*CM SAF CLoud property dAtAset using SEVIRI (CLAAS), edition 2*
summary	*This file contains SEVIRI-based Thematic Climate Data Records (TCDR) produced by the Satellite Application Facility on Climate Monitoring (CM SAF)*
id	*DOI:10.5676/EUM_SAF_CM/CLAAS/V002*
product_version	*2.0*
creator_name	*DE/DWD*
creator_email	*contact.cmsaf@dwd.de*
creator_url	*http://www.cmsaf.eu*
institution	*EUMETSAT/CMSAF*
project	*Satellite Application Facility on Climate Monitoring (CM SAF)*
references	*http://dx.doi.org/10.5676/EUM_SAF_CM/CLAAS/V002*
keywords_vocabulary	*Vocabulary for keywords in the global attributes (GCMD Science Keywords, Version 8.1)*
keywords	*EARTH SCIENCE>ATMOSPHERE>CLOUDS>"variable group"*
Conventions	*convention tables for metadata and attributes (CF-1.6, ACDD-1.3)*
standard_name_vocabulary	*Vocabulary for standard names in the parameter attributes (Standard Name Table (v28, 07 January 2015))*
date_created	*Point in time, when the file was created [ISO8601 date]*
geospatial_lat_max	*90*
geospatial_lat_min	*-90*
geospatial_lat_units	*degrees_north*

Name	Description
geospatial_lon_max	*90*
geospatial_lon_min	*-90*
geospatial_lon_units	*degrees_east*
Geospational_lat_resolution	*0.05 degrees*
Geospational_lon_resolution	*0.05 degrees*
time_coverage_start	*Temporal coverage start of the data [ISO8601 date]*
time_coverage_end	*Temporal coverage end of the data [ISO8601 date]*
time_coverage_duration	*P1M or P1D (period 1 month, day)*
time_coverage_resolution	*P1M or P1D (period 1 month, day)*
platform_vocabulary	*Vocabulary for platform in the global attributes (GCMD Platforms, Version 8.1)*
instrument_vocabulary	*Vocabulary for instrument in the global attributes (GCMD Instruments, Version 8.1)*
instrument	*Earth Remote Sensing Instruments>Passive Remote Sensing >Spectrometers/Radiometers>Imaging Spectrometers/Radiometers>SEVIRI>Spinning Enhanced Visible and Infrared Imager*
CMSAF_included_Daily_Means	*For monthly means, this attribute counts the number of daily means, that are used to build the monthly mean*
CMSAF_area_extent	*-5456233.41938636, -5453233.01608472, 5453233.01608472, 5456233.41938636*
CMSAF_L2_processor	*SAFNWC MSG v2012 with custom CMSAF modifications*
CMSAF_L3_processor	*CMSAFMSGL3_V2.0*
platform	*Earth Observation Satellites > METEOSAT > METEOSAT-8 (or 9 or 10)*

9 Data ordering via the Web User Interface (WUI)

User services are provided through the CM SAF homepage www.cmsaf.eu. The user service includes information and documentation about the CM SAF and the CM SAF products, information on how to contact the user help desk and allows to search the product catalogue and to order products.

On the main webpage, a detailed description how to use the web interface for product search and ordering is given. We refer the user to this description since it is the central and most up to date documentation. However, some of the key features and services are briefly described in the following sections.

9.1 Product ordering process

You need to be registered and logged in to order products. A login is provided upon registration, all products are delivered free of charge. After the selection of the product, the desired way of data transfer can be chosen. This is either via a temporary ftp account (the default setting), or by CD/DVD or email. Each order will be confirmed via email, and the user will get another email once the data have been prepared. If the ftp data transfer was selected, this second email will provide the information on how to access the ftp server.

9.2 Contact User Help Desk staff

In case of questions the contact information of the User Help Desk (e-mail address contact.cmsaf@dwd.de, telephone and fax number) are available via the CM SAF main webpage (http://www.cmsaf.eu) or the main page of the Web User Interface.

9.3 Feedback/User Problem Report

Users of CM SAF products and services are encouraged to provide feedback on the CM SAF product and services to the CM SAF team. Users can either contact the User Help Desk (see chapter 9.2) or use the "User Problem Report" page. A link to the "User Problem Report" is available either from the CM SAF main page (www.cmsaf.eu) or the Web User Interface main page.

9.4 Service Messages / log of changes

Service messages and a log of changes are also accessible from the CM SAF main webpage (www.cmsaf.eu) and provide useful information on product status, versioning and known deficiencies.

10 Copyright and Disclaimer

The user of CM SAF data agrees to respect the following regulations:

Copyright

All intellectual property rights of the CM SAF products belong to EUMETSAT. The use of these products is granted to every interested user, free of charge. If you wish to use these products in publications, presentations, web pages etc., EUMETSAT's copyright credit must be shown by displaying the words "copyright (year) EUMETSAT" on each of the products used.

Acknowledgement and Identification

When exploiting EUMETSAT/CM SAF data you are kindly requested to acknowledge this contribution accordingly and make reference to the CM SAF, e.g. by stating "The work performed was done (i.a.) by using data from EUMETSAT's Satellite Application Facility on Climate Monitoring (CM SAF)". It is highly recommended to clearly identify the product version used. An effective way to do this is the citation of CM SAF data records via the digital object identifier (doi). The doi of the data records can be retrieved through (http://www.cmsaf.eu/DOI).

Re-distribution of CM SAF data

Please do not re-distribute CM SAF data to 3rd parties. The use of the CM SAF products is granted free of charge to every interested user, but we have an essential interest to know how many and what users the CM SAF has. This helps to ensure of the CM SAF operational services as well as its evolution according to user needs and requirements. Each new user shall register at CM SAF in order to retrieve the data.

Feedback

We are keen to learn of what use the CM SAF data are. So please feedback your experiences and your application area of the CM SAF data. EUMETSAT CM SAF is user driven service and is committed to consider the needs and requirements of its users in the planning for product improvements and additions. Users are invited to provide their specific requirements on future products for their applications.

11 References

Berk, A., G. P. Anderson, P. K. Acharya, J. H. Chetwynd, L.S. Bernstein, E. P. Shettle, M. W. Matthew, and S. M. Adler-Golden, 2000: MODTRAN4 Version 2 Users Manual. Technical report, Air Force Materiel Command, Air Force Research Laboratory, Space Vehicles Directorate, Hanscom AFB, MA 01731, USA.

Carbajal Henken, C.K., M.J. Schmeits, H. M. Deneke and R.A. Roebeling, 2011: Using MSG-SEVIRI cloud physical properties and weather radar observations for the detection of Cb/TCu clouds, J. *Appl. Meteor. Climatol*., **50**, 1587–1600, doi: 10.1175/2011JAMC2601.1

Dee et al. (35 named authors), 2011: The ERA-Interim reanalysis: configuration and performance of the data assimilation system, Quart. J. Royal Met. Soc., **137** (656), 553 - 597. Online version: http://onlinelibrary.wiley.com/doi/10.1002/qj.828/abstract.

De Haan, J. F., P. Bosma, and J. W. Hovenier, 1987: The adding method for multiple scattering calculations of polarized light, *Astron. Astrophys*., **183**, 371-391.

Derrien, M. and H. Le Gléau, 2005, MSG/SEVIRI cloud mask and type from SAFNWC, International Journal of Remote Sensing, **26**, No. 21, 4707–4732.

Derrien, M. and H.Le Gléau, 2010: Improvement of cloud detection near sunrise and sunset by temporal differencing and region-growing techniques with real-time SEVIRI, International Journal of Remote Sensing, **31**, No. 7, 1765-1780.

Fuchs, P., 2012: Satellite Application Facility on Climate Monitoring Evaluation Report Change of NWP Input – SEVIRI, SAF/CM/DWD/ER/SEVIRI/1.

Goyens, C., D. Lauwaet, M. Schröder, M. Demuzere, N. van Lipzig, 2011: Tracking Mesoscale Convective Systems in the Sahel: relation between cloud parameters and precipitation, *Int. J. Clim*., doi: 10.1002/joc.2407.

Greuell, W., E. van Meijgaard, J.F. Meirink, and N. Clerbaux, 2011: Evaluation of model predicted top-of-atmosphere radiation and cloud parameters over Africa with observations from GERB and SEVIRI, *J. Climate*, 25, 4015 – 4036, doi:10.1175/2011JCLI3856.1.

Hamann, U., et al., Remote sensing of cloud top pressure/height from SEVIRI: analysis of ten current retrieval algorithms, 2014: *Atmospheric Measurement Techniques*, 7, 2839-2867, doi:10.5194/amt-7-2839-2014.

Haywood, J.M., S.R. Osborne, S.J. Abel, 2004: The effect of overlying absorbing aerosol layers on remote sensing retrievals of cloud effective radius and cloud optical depth, *Quart. J. Roy. Meteorol. Soc*., **130**, 779-800, doi: 10.1256/qj.03.100.

Heidinger, A. K., M. J Foster, A. Walther and X. Zhao, 2013: The Pathfinder Atmospheres Extended (PATMOS-x) AVHRR Climate Data Set., *Bull. Amer. Meteor. Soc*, doi: http://dx.doi.org/10.1175/BAMS-D-12-00246.1.

Hess, H., R. B. A. Koelemeijer, and P. Stammes, 1998: Scattering matrices of imperfect hexagonal crystals. *J. Quant. Spectrosc. Ra*., **60**, 301–308.

Knap, W. H., L. C. Labonnote, G. Brogniez, and P. Stammes, 2005: Modeling total and polarized reflectances of ice clouds: evaluation by means of POLDER and ATSR-2 measurements. *Appl. Optics*, **44**, 4060-4073.

Kuell, V. and A. Bott, 2009: Application of the hybrid convection parameterization scheme HYMACS to different meteorological situations, Atmos. Res., 94, 743-753, doi:10.1016/j.atmosres.2009.04.002.

Maddux, BC, Ackerman, SA, Platnick, S, 2010: Viewing Geometry Dependencies in MODIS Cloud Products, J. Atm. Ocean. Tech., 27(9), 1519-1528.

Meirink, J.F., R.A. Roebeling and P. Stammes, 2009: Atmospheric correction for the KNMI Cloud Physical Properties retrieval algorithm, KNMI publication: TR-304, 17/2/2009, pp22.

Meirink, J.F., R.A. Roebeling and P. Stammes, 2013: Inter-calibration of polar imager solar channels using SEVIRI, Atm. Meas. Tech., 6, 2495-2508, doi:10.5194/amt-6-2495-2013.

Nakajima, T., and M. D. King, 1990: Determination of the Optical Thickness and Effective Particle Radius of Clouds from Reflected Solar Radiation Measurements. Part 1: Theory. *J. Atmos. Sci* ., **47**, 1878-1893.

Pfeifroth, U., R. Hollmann, and B. Ahrens, 2012: Cloud cover diurnal cycles in satellite data and regional climate model simulations, *Meteorologische Zeitschrift*, 21, 551-560.

Platnick, S., 2001: A superposition technique for deriving mean photon scattering statistics in plane-parallel cloudy atmospheres, *J. Quant. Spectrosc. Radiat. Transfer*, **68**, 57-73.

Roebeling, R. A., A. J. Feijt, and P. Stammes, 2006: Cloud property retrievals for climate monitoring: implications of differences between SEVIRI on METEOSAT-8 and AVHRR on NOAA-17, *J. Geophys. Res.*, **111**, D20210, doi:10.1029/2005JD006990.

Roebeling, R. A., and E. van Meijgaard, 2009: Evaluation of the Daylight Cycle of Model-Predicted Cloud Amount and Condensed Water Path over Europe with Observations from MSG SEVIRI, *J. Clim.*, **22** (7), 1749-1766 DOI: 10.1175/2008JCLI2391.1.

Siewert, C. W., M. Koenig and J. R. Mecikalski, 2010: Application of Meteosat second generation data towards improving the nowcasting of convective initiation, *Meteorol. Appl.,* **17**, 4, *DOI 10.1002.*

Stammes, P., 2001: Spectral radiance modeling in the UV-Visible range. IRS 2000: Current problems in Atmospheric Radiation, edited by W.L. Smith and Y.M. Timofeyev, pp 385-388, A. Deepak Publ., Hampton, VA.

Stengel, M., Kniffka, A., Meirink, J. F., Lockhoff, M., Tan, J., and Hollmann, R., 2014: CLAAS: the CM SAF cloud property data set using SEVIRI, *Atmos. Chem. Phys.*, 14, 4297–4311.

Stephens, G. L., 1978: Radiation profiles in extended water clouds: II. Parameterization schemes. *J. Atmos. Sci.*, **35**, 2123-2132.

Trolez, M, K.-G. Karlsson, S. Johnston and P. Albert, 2008: The impact of varying NWP background information on CM-SAF cloud products, CM SAF Visiting Scientist Report, *SMHI Reports Meteorology*, **128**, 41 pp.

Van Weverberg K., van Lipzig N.P.M., Delobbe L., Vogelmann A.M., 2012: The role of precipitation size distributions in km-scale NWP simulations of intense precipitation: evaluation of cloud properties and surface precipitation. *Q. J. R. Meteorol. Soc*. DOI:10.1002/qj.1933.

12 Glossary

AMSR-E	Advanced Microwave Scanning Radiometer for EOS
ATBD	Algorithm Theoretical Baseline Document
AVHRR	Advanced Very High Resolution Radiometer
BC-RMS	Bias-Corrected RMS
CALIPSO	Cloud-Aerosol Lidar and Infrared Pathfinder Satellite Observations
CALIOP	Cloud-Aerosol Lidar with Orthogonal Polarisation
CDO	Climate Data Operators
CDOP	Continuous Development and Operations Phase
CFC	Fractional Cloud Cover
CFOT	Cloud Feature Optical Depth
CLARA-A	CM SAF cLoud, Albedo and Radiation products, AVHRR-based
CLAAS	CM SAF cLoud dAtAset using SEVIRI
CM SAF	Satellite Application Facility on Climate Monitoring
COT	Cloud Optical Thickness
CPH	Cloud Phase
CPR	Cloud Profiling Radar
CTH	Cloud Top Height
CTO	Cloud Top product
CTP	Cloud Top Pressure
CTT	Cloud Top Temperature
CPP	Cloud Physical Properties
DAK	Doubling Adding KNMI (radiative transfer model)
DRR	Delivery Readiness Review
DWD	Deutscher Wetterdienst (German MetService)
ECMWF	European Centre for Medium Range Forecast
ECV	Essential Climate Variable
ERA-Interim	Second ECMWF Re-Analysis data record
EUMETSAT	European Organisation for the Exploitation of Meteorological Satellites
FAR	False Alarm Ratio
FCDR	Fundamental Climate Data Record
FCI	Flexible Combined Imager
GAC	Global Area Coverage (AVHRR)

GCOS	Global Climate Observing System
GSICS	Global Space-Based Inter-Calibration System
ISCCP	International Satellite Cloud Climatology Project
ITCZ	Inter Tropical Convergence Zone
IWP	Ice Water Path
JCH	Joint Cloud properties Histogram
KNMI	Koninklijk Nederlands Meteorologisch Instituut
KSS	Hanssen-Kuiper Skill Score
LWP	Liquid Water Path
MODIS	Moderate Resolution Imaging Spectroradiometer
MSG	Meteosat Second Generation
MTG	Meteosat Third Generation
NOAA	National Oceanic & Atmospheric Administration
NWC SAF	SAF on Nowcasting and Very Short Range Forecasting
NWP	Numerical Weather Prediction
PATMOS-x	Pathfinder Atmospheres-Extended dataset (NOAA)
POD	Probability Of Detection
PPS	Polar Platform System (NWC SAF polar cloud software package)
PRD	Product Requirement Document
PUM	Product User Manual
REFF	Cloud particle effective radius
RMS	Root Mean Square (Error)
RTTOV	Radiative Transfer model for TOVS
SEVIRI	Spinning Enhanced Visible and InfraRed Imager
SAF	Satellite Application Facility
SMHI	Swedish Meteorological and Hydrological Institute
SYNOP	Synoptic observations
SZA	Solar Zenith Angle
UWisc	University of Wisconsin passive microwave based LWP dataset
VZA	Viewing Zenith Angle